DOI: 10.1007/s11099-012-0014-x PHOTOSYNTHETICA 50 (1): 141-151, 2012

Acclimation of photosynthesis in a boreal grass (*Phalaris arundinacea* L.) under different temperature, CO_2, and soil water regimes

Z.-M. GE[*,**,+], X. ZHOU[**], S. KELLOMÄKI[**], C. ZHANG[**], H. PELTOLA[**], P.J. MARTIKAINEN[***], and K.Y. WANG[**]

State Key Laboratory of Estuarine and Coastal Research, East China Normal University, 3663 Zhongshan Road North, 200062 Shanghai, China[*]
School of Forest Sciences, University of Eastern Finland, Yliopistokatu 7, P.O. Box 111, 80101 Joensuu, Finland[**]
Department of Environmental Science, University of Eastern Finland, P.O. Box 1627, 70211 Kuopio, Finland[***]

Abstract

The aim of this work was to study the acclimation of photosynthesis in a boreal grass (*Phalaris arundinacea* L.) grown in controlled environment chambers under elevated temperature (ambient + 3.5°C) and CO_2 (700 μmol mol^{-1}) with varying soil water regimes. More specifically, we studied, during two development stages (early: heading; late: florescence completed), how the temperature response of light-saturated net photosynthetic rate (P_{sat}), maximum rate of ribulose-1,5-bisphosphate carboxylase/oxygenase activity (V_{cmax}) and potential rate of electron transport (J_{max}) acclimatized to the changed environment. During the early growing period, we found a greater temperature-induced enhancement of P_{sat} at higher measurement temperatures, which disappeared during the late stage. Under elevated growth temperature, V_{cmax} and J_{max} at lower measurement temperatures (5–15°C) were lower than those under ambient growth temperature during the early period. When the measurements were done at 20–30°C, the situation was the opposite. During the late growing period, V_{cmax} and J_{max} under elevated growth temperature were consistently lower across measurement temperatures. CO_2 enrichment significantly increased P_{sat} with higher intercellular CO_2 compared to ambient CO_2 treatment, however, elevated CO_2 slightly decreased V_{cmax} and J_{max} across measurement temperatures, probably due to down-regulation acclimation. For two growing periods, soil water availability affected the variation in photosynthesis and biochemical parameters much more than climatic treatment did. Over two growing periods, V_{cmax} and J_{max} were on average 36.4 and 30.6%, respectively, lower with low water availability compared to high water availability across measurement temperatures. During the late growing period, elevated growth temperature further reduced the photosynthesis under low water availability. V_{cmax} and J_{max} declined along with the decrease in nitrogen content of leaves as growing period progressed, regardless of climatic treatment and water regime. We suggest that, for grass species, seasonal acclimation of the photosynthetic parameters under varying environmental conditions needed to be identified to fairly estimate the whole-life photosynthesis.

Additional key words: acclimation of photosynthesis; carbon dioxide; carboxylation efficiency; electron transport; temperature; water deficit.

Received 12 April 2011, *accepted* 9 January 2012.
[+]Corresponding author; tel.: +358-13-251-4441, fax: +358-13-251-4444, e-mail: zhenming.ge@uef.fi
Abbreviations: C_a – CO_2 concentration; C_c – chloroplast CO_2 concentration; C_i – intercellular CO_2 concentration; CON – ambient environment in chamber; EC – elevated CO_2 concentration in chamber; ET – elevated temperature in chamber; ETC – chamber with combination of temperature and CO_2 elevation; g_m – mesophyll conductance; g_{sat} – light-saturated stomatal conductance; ΔH_a – enthalpy of activation; ΔH_d – enthalpy of deactivation; J – rate of electron transport; J_{max} – maximum rate of electron transport; K_c, K_o – Rubisco Michaelis constants for CO_2, O_2; N_L– nitrogen content based on leaf area; O – O_2 concentration; P_c – Rubisco-limited rate of photosynthesis; P_j – RuBP-regeneration-limited rate of photosynthesis; P_N – net photosynthetic rate; P_{sat} – light-saturated net photosynthetic rate; PPFD – photosynthetic photon flux densities; R – molar gas constant; RCG – reed canary grass; R_d – mitochondrial respiration in light; ΔS– entropy of the desaturation equilibrium; T_{opt} – optimal temperature; V_{cmax} – maximum rate of carboxylation by Rubisco; α – quantum efficiency; Γ^* – CO_2 compensation point (absence of dark respiration); θ – curvature of the light-response curve.
Acknowledgments: This work was funded through the Finland Distinguished Professor Programme (FiDiPro) of the Academy of Finland (No. 127299-A5060-06) and the Finnish Network Graduate School in Forest Sciences of the Academy of Finland (No. 49996). Thanks are due to Matti Turpeinen of *Vapo Ltd*. for providing relevant logistical information on the field sites. The controlled environment chamber system was funded by European Regional Development Fund (ERDF) granted by the State Provincial Office of Eastern Finland. Matti Lemettinen, Alpo Hassinen, Risto Ikonen and Eine Ihanus at the Mekrijärvi Research Station, are thanked for their technical assistance. Dr. David Gritten is greatly thanked for revising the language of this paper.

Introduction

Numerous studies have been conducted to understand the acclimated photosynthetic response of C_3 plants to rising growth temperature and CO_2 (Bernacchi *et al*. 2001, 2002; Long *et al*. 2004, Pérez *et al*. 2007) and water stress (Flexas 2004a,b; Hu *et al*. 2010). In this regard, the maximum rate of ribulose-1,5-bisphosphate carboxylase/oxygenase (Rubisco) activity (V_{cmax}) and the potential rate of electron transport (J_{max}) are two core parameters indicating the Rubisco-limited photosynthesis and the RuBP-regeneration-limited photosynthesis, respectively (Sharkey *et al*. 2007).

Based on the literature, the short-term temperature responses of V_{cmax} and J_{max} under high growth temperature are likely to increase or decrease depending on species, phenology and the growing conditions (Bernacchi *et al*. 2001, Medlyn *et al*. 2002a,b; Urban *et al*. 2007). The acclimated response to CO_2 enrichment is also evident but equally variable, *i.e*., it may decrease (Long *et al*. 2004, Zhang *et al*. 2009) or increase (Alonso *et al*. 2008, 2009) the photosynthetic parameters. Consequently, the widely used biochemical photosynthesis model in terms of V_{cmax} and J_{max}, which has been developed by Farquhar *et al*. (1980) and Farquhar and von Caemmerer (1982), provides a means to study the photosynthetic response of C_3 plants and possible acclimation of photosynthesis to climate change in the long run (Medlyn *et al*. 2002a,b).

The response of photosynthetic capacity to environmental conditions during different growing periods may represent the variations of photosynthetic acclimation (Pérez *et al*. 2007, Gouasmi *et al*. 2009, Ge *et al*. 2011). This information is needed to better understand how the key photosynthetic parameters acclimate to the varying growth conditions in order to predict the continuous carbon uptake over the growing season. This is especially the case for the boreal herbaceous plants with short life cycles, such as reed canary grass (*Phalaris arundinacea* L., here after RCG), which is a common perennial C_3 grass in North Europe. Recently in Finland and Sweden, the cultivation area of this plant as a bioenergy crop has rapidly increased (Sahramaa and Jauhiainen 2003, Zhou *et al*. 2011). However, little is known about its physiological and growth responses to varying climatic treatments and availability of soil water (Ge *et al*. 2011, 2012; Zhou *et al*. 2011).

In this context, an experiment was conducted to study the acclimation of photosynthesis of RCG plants, grown in controlled environment chambers over two growing seasons (2009–2010), to elevated growth temperature and CO_2 with different soil water availability. Specifically, we had the following study aims: (*1*) to identify the acclimation of the temperature dependency of carboxylation efficiency and electron transport capacity, under given climatic treatments and water regimes, and (*2*) to validate the predicted photosynthesis against a set of measurements during two development stages.

Materials and methods

Experimental design: In 2009, 48 microcosms consisting of organic soil monoliths (0.8 m × 0.6 m × 0.4 m, sufficient volume for root growth) with RCG plants were cored from the Linnansuo peatland (62°30'N, 30°30' E, belonging to *Vapo Bioenergy Ltd*.) in eastern Finland. RCG plants were cultivated from April 2009 until September 2010 in the controlled environment greenhouse system at the Mekrijärvi Research Station (62°47'N, 30°58'E, belonging to the University of Eastern Finland). The plants were fertilized with 5.4 g(N) m^{-2}, 1.2 g(P) m^{-2} and 4.2 g(K) m^{-2} during each year applying the management practices used by *Vapo Bioenergy Ltd*.

The greenhouse system consists of 16 chambers working independently with four replicates for each climatic treatment: (*1*) ambient temperature and CO_2 concentration (CON); (*2*) elevated temperature and ambient CO_2 concentration (ET); (*3*) elevated CO_2 concentration and ambient temperature (EC); and (*4*) elevated temperature and CO_2 concentration (ETC). During the period of RCG cultivation (2009−2010), the CON chambers were set to follow the outside free air temperature and CO_2 concentration (around 370 μmol mol^{-1}) (climatic datum see Zhou *et al*. 2011). In the elevated-temperature chambers (ET and ETC), the target temperature was set at +3.5°C above that in the CON chambers. The target CO_2 concentration in the elevated CO_2 chambers (EC and ETC) was set at 700 μmol mol^{-1}. All of the chambers received the ambient irradiance throughout the trial, while the air relative humidity inside was set more than 50% with an adjustable humidifier. The technical details and performance of the chambers have been described in detail by Zhou *et al*. (2012).

Each chamber contained three RCG containers treated with three soil water regimes (soil moisture content), ranging from high (HW, 100% volumetric soil water content), to normal (NW, ~50%, roughly same as field measurement) and low (LW, ~30%). Soil moisture was monitored with soil moisture sensors (*Theta Probe ML 1*, *Delta-T Devices*, Cambridge, UK) to keep the soil moisture at the target level through irrigation.

Measurement layout of leaf gas exchange: The gas-exchange measurements were conducted with a 2 cm × 3 cm standard leaf cuvette in a portable steady-state photosynthesis system (*Li-6400, Li-cor Inc*., Nebraska,

USA) during two plant development stages in 2010: the first period in 10th–25st June (GP-I, heading) and the second one 1st–15th August (GP-II, florescence completed: branches of inflorescence closed along the rachis, seed ripening). Measurements were performed on the intact, second fully expanded leaves from 08:00 to 11:00 h on sunny and cloud-free days. The leaf area was measured using a leaf area meter (*Li-3100, Li-cor Inc*., Nebraska, USA). Four plants in each container in each chamber were measured for replicates.

***P*sat and *g*sat**: The measurements of temperature response of light-saturated net photosynthetic rate (P_{sat}) and light-saturated stomatal conductance (g_{sat}) were done at 5°C intervals from 5 to 30°C for leaf temperature, under 1,500 μmol m^{-2} s^{-1} photosynthetic photon flux densities (PPFD). The air flow in the leaf chamber was set at 400 ml min^{-1}, the vapour pressure deficit was kept at 1.0 ± 0.1 kPa, and relative humidity of the air in the leaf chamber was set above 60%. The CO_2 source for the measurements was a computer-controlled CO_2 mixing system supplied with the *Li-6400*. The CO_2 concentration was kept at 370 ± 1 μmol mol^{-1} in the CON and ET chambers and 700 ± 2 μmol mol^{-1} in the EC and ETC chambers.

***V*cmax and *J*max**: From 5 to 30°C for leaf temperature, the response of net photosynthetic rate (P_N) to intercellular CO_2 concentration (C_i) and PPFD were measured at intervals of 5°C. The P_N-C_i and P_N-PPFD response curves were used to estimate V_{cmax}, mitochondrial respiration in light (R_d), and quantum efficiency (α) and rate of electron transport (J), respectively (Eqs. 2–4 in Appendix). And then, J_{max} were calculated as the value of J at light-saturated (Eq. 5 in Appendix). The variability of mesophyll conductance (g_m) was also obtained through P_N-C_i curves, using the curve-fitting calculator developed by Sharkey *et al*. (2007). The P_N-C_i curves were carried out under saturating light intensity [1,500 μmol(photon) m^{-2} s^{-1}]. The CO_2 concentration in the leaf chamber was lowered in a stepwise manner from 370 to 20 μmol mol^{-1} (including 6–7 points) and then returned to 370 μmol mol^{-1} to re-establish the initial steady state value of photosynthesis. Thereafter C_a was increased steadily from 370 to 1,400 μmol mol^{-1} (including 5–6 points). Gas-exchange measurements were determined as soon as the inlet air CO_2 concentration was stable (Long and Bernacchi 2003). The P_N-PPFD curves were carried out under 1,400 μmol mol^{-1}(CO_2) concentration by reducing, in a stepwise manner, the value of PPFD from 1,500 to 20 μmol m^{-2} s^{-1} (including 10–11 points). Sufficient time was allowed for photosynthesis to stabilize to the new PPFD before logging the measurements (typically requiring 10 min or less). The leaves were allowed to equilibrate for 20 min before logging the data in the P_N-C_i and P_N-PPFD curves.

Leaf nitrogen content: After gas-exchange measurement, the measured leaves were dried in a forced-air oven (70°C, 72 h) to determine the dry mass. The dried leaves were then ground and sieved for analyzing the content of leaf nitrogen (N_L) using an Elemental Vario Micro Cube CHNS analyzer (*Elementar Analysensysteme GmbH*, Germany). The values of N_L were expressed on a leaf-area basis.

Farquhar's model and photosynthetic parameters: As demonstrated in the biochemical model of Farquhar *et al*. (1980) and Farquhar and von Caemmerer (1982), the P_N-C_i and P_N-PPFD curves describe three phases: (*1*) when C_i is at a lower/moderate level, P_N is determined by the efficiency of Rubisco enzyme system; (*2*) with the increase in C_i, P_N is limited by RuBP-regeneration; and (*3*) a further increase in C_i may result in a plateau or a decrease in P_N if triose-phosphate utilization (TPU) becomes limiting (Long and Bernacchi 2003). Most often, TPU-limitation is not apparent at any C_i and so only two phases may be seen (Long and Bernacchi 2003, Sharkey *et al*. 2007). Accordingly, in this study, the emphasis was on the Rubisco-limited and the RuBP-regeneration-limited photosynthesis in terms of the parameter estimation of V_{cmax} and J_{max} (Eqs. 2–5 in Appendix).

Statistical analysis and validation of photosynthesis model: Statistical analyses were carried out using the *SPSS 16.0* (Chicago, IL, USA) software package. Regarding the values of the physiological parameters, the effects of various treatments were tested (temperature, CO_2 and soil water availability) including their interactions using the three-way *ANOVA*. Differences between treatments were assessed to be statistically significant at $p<0.05$. Furthermore, the mean differences of physiological parameters among the four climate chamber treatments (CON, ET, EC, and ETC) and three soil water regimes at two growing periods (GP-I and GP-II) were tested using *Tukey*'s HSD test.

In the validation work of the photosynthesis model, we compared the predicted P_{sat} against a set of measurements of P_{sat} not used in the parameter estimation. In this work, the estimated V_{cmax} and J_{max} were entered into Eqs. 1–6 to calculate P_{sat} at different leaf temperatures (5–30°C) during two growing periods, for plants grown under different climatic treatments and water regimes.

Results

Temperature dependence of *P*sat and *g*sat: During both growing periods (GP-I and GP-II), P_{sat} and g_{sat} displayed a curvilinear response to the measurement temperatures regardless of growth environment (climatic treatments

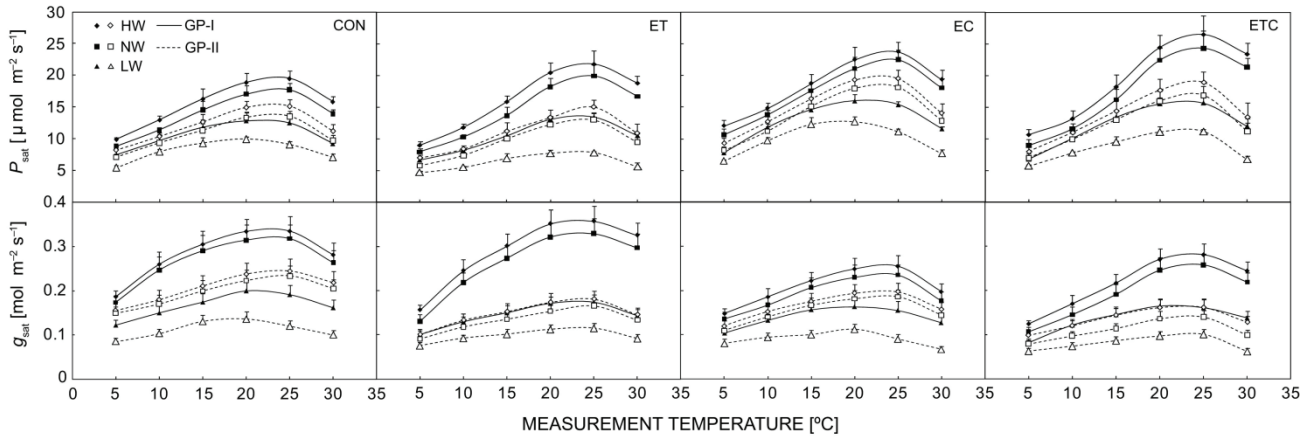

Fig. 1. Means (± SE, n=4) of the light-saturated net photosynthetic rates (P_{sat}) and the light-saturated stomatal conductance (g_{sat}) in the CON, ET, EC and ETC chambers with different water regimes (HW, NW, and LW) at different measurement temperatures (5–30°C) during GP-I (*solid line*) and GP-II (*dashed line*), based on four replicates in each climate treatment.

and water regimes) (Fig. 1). P_{sat} and g_{sat} were significantly (p<0.05) lower during GP-II compared to GP-I, across the measurement temperatures (Fig. 1, Table 1), regardless of climatic treatment and water regime. The differences between measurement periods, CO_2 levels, and water regimes were significant (p<0.05) for P_{sat} and g_{sat} (Table 2), this was also the case for the effect of growth temperature and the interactions between CO_2 level × water regime for g_{sat}.

During GP-I, P_{sat} and g_{sat} at the lower measurement temperatures of 5–15°C, were, on average, 11.2 and 12.0% lower under elevated growth temperature (ET and ETC) compared to ambient growth temperature (CON and EC), respectively regardless of water regime. When the measurements were done at 20–30°C, the situation was the opposite, *i.e.*, P_{sat} and g_{sat} were, on average, 11.8 and 6% higher under elevated growth temperature, respectively (Table 1). During GP-II, P_{sat} and g_{sat}, under elevated growth temperature, were on average 12.4 and 21.8% lower compared to ambient growth temperature, respectively, across the measurement temperatures (Table 1), regardless of water regime. Over two growing stages, CO_2 enrichment (EC and ETC) significantly (p<0.05) increased P_{sat} and decreased g_{sat} compared to ambient CO_2 (CON and ET) across the measurement temperatures (Fig. 1, Table 1), regardless of water regime.

P_{sat} and g_{sat} were, on average, 31.0 and 37.8% lower (p<0.05) in LW compared to HW and NW, respectively (Fig. 1, Table 1), regardless of growing period and climatic treatment. During GP-II, P_{sat} and g_{sat} showed the lowest values across the measurement temperatures in LW under elevated growth temperature compared to ambient growth temperature (Fig. 1).

Temperature dependence of V_{cmax} and J_{max}: Regardless of growth condition and growing period, V_{cmax} and J_{max} peaked around the measurement temperature of 25°C, and then declined with the increases in measurement temperature (Fig. 2). V_{cmax} and J_{max} were significantly (p<0.05) lower during GP-II compared to GP-I (Fig. 2, Table 1), regardless of climatic treatment and water regime. The effects of measurement periods and water regimes on V_{cmax} and J_{max} were significant (p<0.05) (Table 2).

During GP-I, V_{cmax} and J_{max} at 5–15°C, were on average 10.7% and 5.6% lower under elevated growth temperature compared to ambient growth temperature, respectively (Table 1), regardless of water regime. When the measurements were done at 20–30°C, the situation was the opposite with higher V_{cmax} and J_{max} by 5.6% and 15.8%, respectively. During GP-II, V_{cmax} and J_{max}, under elevated growth temperature, were lower by on average 14.7% and 8.9%, respectively (Table 1), compared to ambient growth temperature, across the measurement temperatures regardless of water regime.

The normalized (to 1 at 25°C) temperature responses of V_{cmax} and J_{max} are shown in Fig. 3. Elevated growth temperature shifted the optimum temperature of the parameters to higher temperatures, regardless of water regime. During GP-I, the optimum temperature for V_{cmax} was 24.5–27.6°C and 20.0–23.2°C, and for J_{max} 22.3–25.6°C and 18.2–21.0°C under elevated growth temperature and ambient growth temperature, respectively (Fig. 2). During GP-II, the optimum temperature for both parameters was not significantly changed under elevated growth temperature (Fig. 2).

Over GP-I and GP-II, elevated CO_2 slightly reduced V_{cmax} and J_{max}, on average, by 9.3% and 5.0% compared to ambient CO_2, respectively, across the measurement temperatures regardless of water regime (Fig. 2, Table 1). The effect of CO_2 enrichment on the optimum temperature for V_{cmax} and J_{max} was not significant (Fig. 3), regardless of growth temperature and water regime.

Over GP-I and GP-II, V_{cmax} and J_{max} were, on average, 36.4% and 30.6% lower (p<0.05) in LW compared to HW and NW, respectively, regardless of climatic treatment (Fig. 2, Table 1). LW shifted the optimum temperature of parameters to lower temperatures (Fig. 3), regardless of climatic treatment. During both measurement

Table 1. Means (± SE, n=4) of light-saturated net photosynthetic rate (P_{sat}), light-saturated stomatal conductance (g_{sat}), maximum rate of carboxylation (V_{cmax}), maximum rate of electron transport (J_{max}) and ratio of J_{max}/V_{cmax} in the climate chambers (CON, ET, EC, and ETC) with different water regimes (HW, NW, and LW) at measurement temperature of 25°C during GP-I and GP-II, based on four replicates in each climate treatment. Different *uppercase letters* denote significant differences among means within each column (p<0.05, *Tukey*'s HSD test).

Climatic treatments	Water regimes	P_{sat} [μmol m^{-2} s^{-1}]		g_{sat} [mol m^{-2} s^{-1}]		V_{cmax} [μmol m^{-2} s^{-1}]		J_{max} [μmol m^{-2} s^{-1}]		J_{max}/V_{cmax}	
		GP-I	GP-II	GP-I	GP-II	GP-I	GP-II	GP-I	GP-II	GP-I	GP-II
CON	HW	19.5 ± 1.2^{b}	15.1 ± 1.0^{bc}	0.34 ± 0.02^{a}	0.24 ± 0.02^{a}	83.9 ± 6.8^{a}	62.9 ± 5.0^{a}	150.6 ± 11.8^{ab}	113.5 ± 8.6^{a}	1.8 ± 0.2^{b}	1.8 ± 0.2^{b}
	NW	17.7 ± 1.0^{bc}	13.5 ± 0.9^{c}	0.32 ± 0.02^{ab}	0.23 ± 0.02^{a}	77.0 ± 6.2^{ab}	57.4 ± 4.5^{a}	143.9 ± 11.1^{b}	102.0 ± 7.7^{ab}	1.9 ± 0.2^{b}	1.8 ± 0.2^{b}
	LW	12.5 ± 0.6^{d}	9.0 ± 0.5^{de}	0.19 ± 0.02^{d}	0.12 ± 0.01^{cd}	38.5 ± 2.8^{c}	29.5 ± 2.0^{c}	91.6 ± 8.9^{c}	67.0 ± 6.8^{c}	2.4 ± 0.3^{a}	2.3 ± 0.3^{a}
ET	HW	21.8 ± 2.1^{b}	15.0 ± 1.2^{bc}	0.36 ± 0.04^{a}	0.18 ± 0.02^{b}	85.3 ± 6.9^{a}	54.1 ± 4.2^{ab}	173.2 ± 19.3^{a}	106.2 ± 11.5^{a}	2.0 ± 0.3^{ab}	2.0 ± 0.3^{ab}
	NW	20.0 ± 1.8^{b}	13.0 ± 1.0^{c}	0.33 ± 0.03^{ab}	0.17 ± 0.02^{b}	78.1 ± 6.3^{ab}	48.8 ± 3.7^{b}	161.6 ± 17.1^{a}	95.0 ± 10.0^{ab}	2.1 ± 0.3^{ab}	1.9 ± 0.3^{b}
	LW	13.4 ± 0.7^{cd}	7.8 ± 0.3^{e}	0.17 ± 0.02^{de}	0.11 ± 0.01^{d}	42.9 ± 3.2^{c}	26.5 ± 1.8^{cd}	97.2 ± 10.2^{c}	66.1 ± 5.8^{c}	2.3 ± 0.3^{a}	2.5 ± 0.3^{a}
EC	HW	23.8 ± 1.6^{ab}	19.5 ± 1.4^{a}	0.24 ± 0.02^{c}	0.20 ± 0.02^{ab}	81.0 ± 6.3^{a}	59.6 ± 4.6^{a}	145.9 ± 17.2^{b}	108.1 ± 10.3^{a}	1.8 ± 0.3^{b}	1.8 ± 0.2^{b}
	NW	22.5 ± 1.5^{ab}	18.1 ± 1.3^{ab}	0.24 ± 0.03^{c}	0.19 ± 0.01^{b}	72.2 ± 5.9^{ab}	54.9 ± 4.1^{ab}	137.4 ± 15.6^{b}	97.3 ± 9.3^{ab}	1.9 ± 0.3^{b}	1.8 ± 0.2^{b}
	LW	15.4 ± 0.5^{c}	11.1 ± 0.3^{cd}	0.14 ± 0.02^{e}	0.09 ± 0.01^{e}	35.4 ± 2.4^{cd}	28.5 ± 1.8^{c}	84.5 ± 8.3^{cd}	66.2 ± 4.8^{c}	2.4 ± 0.3^{a}	2.3 ± 0.3^{a}
ETC	HW	26.5 ± 3.0^{a}	18.9 ± 1.7^{a}	0.28 ± 0.03^{bc}	0.16 ± 0.03^{bc}	84.3 ± 6.6^{a}	52.2 ± 3.9^{ab}	168.7 ± 12.7^{a}	101.6 ± 9.4^{ab}	2.0 ± 0.2^{ab}	1.9 ± 0.2^{b}
	NW	24.3 ± 2.8^{a}	16.9 ± 1.5^{b}	0.26 ± 0.03^{bc}	0.14 ± 0.02^{c}	75.7 ± 5.9^{ab}	44.6 ± 3.2^{b}	152.4 ± 12.1^{ab}	92.3 ± 8.4^{b}	2.0 ± 0.2^{ab}	2.1 ± 0.3^{ab}
	LW	15.6 ± 1.5^{c}	11.1 ± 0.4^{cd}	0.15 ± 0.02^{e}	0.10 ± 0.01^{de}	39.7 ± 2.8^{c}	26.0 ± 1.6^{cd}	92.7 ± 7.5^{c}	56.0 ± 5.3^{d}	2.3 ± 0.3^{a}	2.2 ± 0.3^{ab}

Table 3. Mean (± SE, n=4) estimates of model parameters used to describe the temperature dependency of V_{cmax} and J_{max} with Eq. 6 over a range of temperature (5–30°C) in the climate chambers (CON, ET, EC and ETC) with different water regimes (HW, NW and LW) during GP-I and GP-II. ΔH_a is the enthalpy of activation, ΔH_d is the enthalpy of deactivation, and ΔS is the entropy of the desaturation equilibrium. Different upper case letters denote significant differences among means within each column (p<0.05, *Tukey*'s HSD test).

Climatic treatments	Water regimes	For V_{cmax} ΔH_a [kJ mol^{-1}]		ΔH_d [kJ mol^{-1}]		ΔS [kJ K^{-1} mol^{-1}]		For J_{max} ΔH_a [kJ mol^{-1}]		ΔH_d [kJ mol^{-1}]		ΔS [kJ K^{-1} mol^{-1}]	
		GP-I	GP-II	GP-I	GP-II	GP-I	GP-II	GP-I	GP-II	GP-I	GP-II	GP-I	GP-II
CON	HW	44.7 ± 2.3^{b}	42.2 ± 2.2^{a}	200.3 ± 19^{a}	198.9 ± 19^{a}	0.67 ± 0.06^{a}	0.67 ± 0.05^{a}	31.9 ± 3.2^{a}	19.3 ± 1.8^{a}	200.7 ± 20^{a}	201.4 ± 19^{a}	0.67 ± 0.06^{a}	0.67 ± 0.07^{a}
	NW	42.1 ± 3.1^{b}	41.1 ± 2.5^{a}	200.2 ± 23^{a}	199.2 ± 20^{a}	0.67 ± 0.06^{a}	0.66 ± 0.06^{a}	31.8 ± 2.9^{a}	19.3 ± 2.1^{a}	200.9 ± 20^{a}	201.2 ± 20^{a}	0.67 ± 0.07^{a}	0.67 ± 0.07^{a}
	LW	17.8 ± 2.0^{de}	17.1 ± 1.9^{bc}	200.5 ± 21^{a}	199.1 ± 15^{a}	0.66 ± 0.05^{a}	0.66 ± 0.04^{a}	14.2 ± 2.9^{d}	13.0 ± 1.0^{bc}	201.0 ± 19^{a}	201.5 ± 21^{a}	0.66 ± 0.07^{a}	0.67 ± 0.06^{a}
ET	HW	56.7 ± 3.6^{a}	38.8 ± 3.5^{a}	200.7 ± 22^{a}	198.5 ± 18^{a}	0.66 ± 0.06^{a}	0.66 ± 0.06^{a}	34.0 ± 3.4^{a}	18.8 ± 2.0^{a}	200.9 ± 19^{a}	201.2 ± 23^{a}	0.66 ± 0.06^{a}	0.66 ± 0.05^{a}
	NW	54.7 ± 3.2^{a}	37.9 ± 3.7^{ab}	200.5 ± 21^{a}	198.9 ± 18^{a}	0.66 ± 0.07^{a}	0.66 ± 0.05^{a}	32.1 ± 3.0^{a}	16.9 ± 1.7^{ab}	200.7 ± 20^{a}	201.4 ± 21^{a}	0.66 ± 0.05^{a}	0.66 ± 0.06^{a}
	LW	29.5 ± 2.8^{cd}	13.5 ± 1.4^{cd}	200.7 ± 22^{a}	199.2 ± 19^{a}	0.66 ± 0.05^{a}	0.66 ± 0.06^{a}	19.5 ± 2.0^{c}	12.5 ± 1.3^{c}	201.0 ± 18^{a}	201.5 ± 20^{a}	0.66 ± 0.06^{a}	0.66 ± 0.05^{a}
EC	HW	42.5 ± 3.4^{b}	40.4 ± 3.4^{a}	199.3 ± 20^{a}	199.0 ± 18^{a}	0.67 ± 0.06^{a}	0.67 ± 0.04^{a}	23.6 ± 2.3^{b}	18.8 ± 1.6^{a}	200.9 ± 15^{a}	201.2 ± 19^{a}	0.67 ± 0.07^{a}	0.67 ± 0.06^{a}
	NW	40.5 ± 2.7^{bc}	39.9 ± 3.3^{a}	199.2 ± 20^{a}	199.0 ± 21^{a}	0.67 ± 0.05^{a}	0.67 ± 0.05^{a}	22.9 ± 2.8^{b}	17.5 ± 1.5^{ab}	200.7 ± 19^{a}	201.4 ± 18^{a}	0.67 ± 0.05^{a}	0.67 ± 0.04^{a}
	LW	16.6 ± 1.8^{e}	15.5 ± 1.4^{c}	199.2 ± 23^{a}	199.2 ± 20^{a}	0.66 ± 0.05^{a}	0.66 ± 0.06^{a}	13.6 ± 1.8^{d}	12.6 ± 1.1^{c}	201.0 ± 20^{a}	201.5 ± 19^{a}	0.67 ± 0.06^{a}	0.67 ± 0.07^{a}
ETC	HW	53.2 ± 3.6^{a}	37.8 ± 3.8^{ab}	199.3 ± 18^{a}	199.1 ± 20^{a}	0.66 ± 0.06^{a}	0.66 ± 0.06^{a}	25.3 ± 2.8^{b}	15.0 ± 1.6^{b}	200.9 ± 17^{a}	201.4 ± 20^{a}	0.66 ± 0.07^{a}	0.67 ± 0.05^{a}
	NW	53.2 ± 3.1^{a}	37.1 ± 3.2^{ab}	199.3 ± 17^{a}	199.7 ± 16^{a}	0.66 ± 0.06^{a}	0.66 ± 0.06^{a}	21.1 ± 2.0^{bc}	15.0 ± 1.3^{b}	200.7 ± 18^{a}	201.2 ± 20^{a}	0.66 ± 0.05^{a}	0.66 ± 0.06^{a}
	LW	27.7 ± 2.2^{cd}	12.7 ± 1.2^{cd}	199.4 ± 19^{a}	199.0 ± 18^{a}	0.66 ± 0.06^{a}	0.66 ± 0.07^{a}	14.1 ± 1.7^{d}	9.5 ± 1.1^{cd}	201.0 ± 20^{a}	201.5 ± 19^{a}	0.66 ± 0.06^{a}	0.66 ± 0.07^{a}

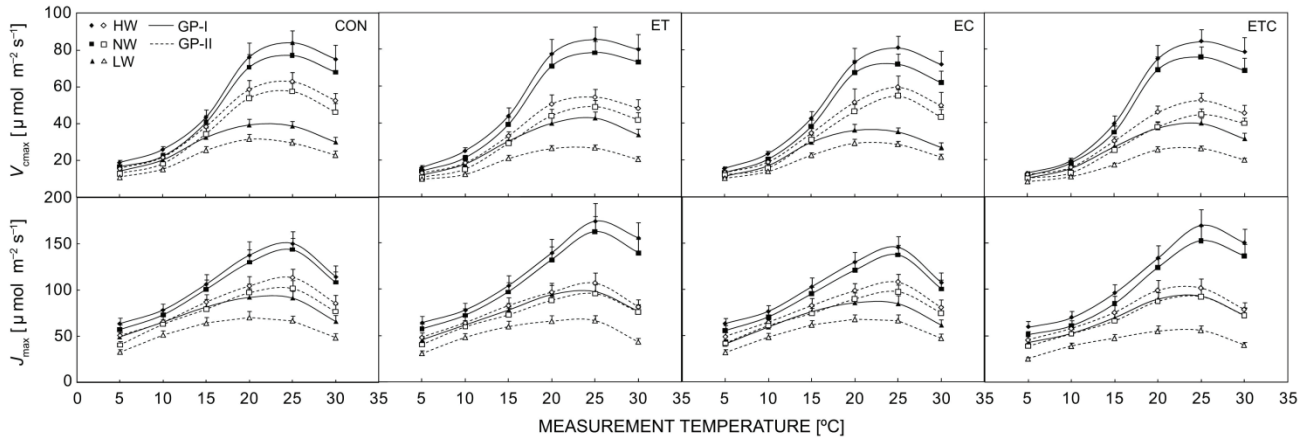

Fig. 2. Means (± SE, n=4) of the maximum rate of ribulose-1,5-bisphosphate carboxylase/oxygenase activity (V_{cmax}) and the potential rate of electron transport (J_{max}) in the CON, ET, EC, and ETC chambers with different water regimes (HW, NW, and LW) at different measurement temperatures (5–30°C) during GP-I (*solid line*) and GP-II (*dashed line*), based on four replicates in each climate treatment.

Table 2. *ANOVA* (F probability) of light-saturated net photosynthetic rate (P_{sat}), light-saturated stomatal conductance (g_{sat}), maximum rate of carboxylation (V_{cmax}) and maximum rate of photosynthetic electron transport (J_{max}), with the variances of growing periods (GP), growth temperature (T), growth CO_2 (CO_2) and water regimes (W). * – p<0.05 (significant); ns – nonsignificant.

Variances	P_{sat} [μmol m^{-2} s^{-1}]		g_{sat} [mol m^{-2} s^{-1}]		V_{cmax} [μmol m^{-2} s^{-1}]		J_{max} [μmol m^{-2} s^{-1}]		J_{max}/V_{cmax}	
	F	p	F	p	F	p	F	p	F	p
GP	174.9	*	268.5	*	76.9	*	164.2	*	4.4	ns
T	3.1	ns	23.9	*	2.5	ns	0.0	ns	5.8	ns
CO_2	100.8	*	79.0	*	3.1	ns	6.0	ns	1.4	ns
W	133.8	*	149.3	*	79.1	*	100.8	*	7.1	*
T × CO_2	0.0	ns	2.1	ns	0.1	ns	0.3	ns	0.1	ns
T × W	1.0	ns	1.0	ns	0.1	ns	0.3	ns	0.2	ns
CO_2 × W	2.3	ns	7.5	*	0.1	ns	0.0	ns	0.2	ns
T × CO_2 × W	0.2	ns	0.0	ns	0.1	ns	0.1	ns	0.1	ns

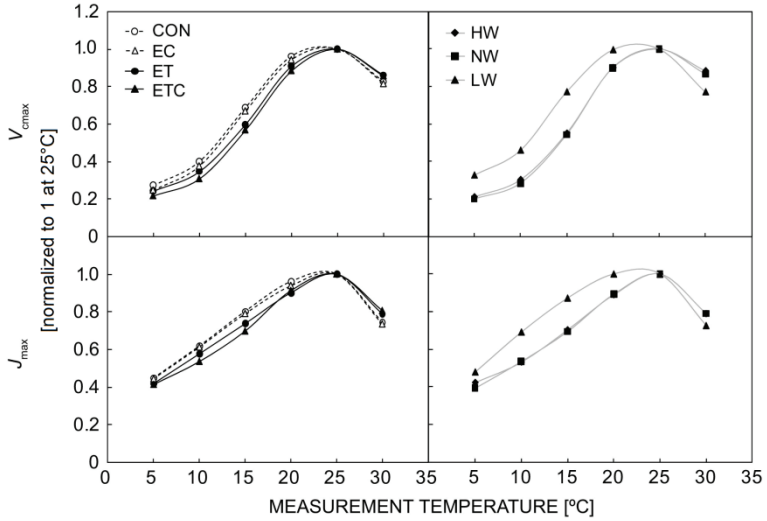

Fig. 3. Temperature responses of the maximum rate of ribulose-1,5-bisphosphate carboxylase/oxygenase activity (V_{cmax}) and the potential rate of electron transport (J_{max}) for climatic treatments (CON, ET, EC, and ETC; over water regimes) and water regimes (HW, NW, and LW; over climatic treatments) over GP-I and GP-II. Values are normalized to 1 at 25ºC.

periods, N_L was significantly (p<0.05) lower in LW compared to HW and NW (Fig. 4). From GP-I to GP-II, N_L decreased, on average, by 38, 40, and 56% for HW, NW, and LW, respectively, over the climatic treatments, and V_{cmax} and J_{max} at 25°C declined along with the decreases in N_L (Fig. 4).

Validation on photosynthesis model: The predicted P_{sat}

based on the photosynthesis model and the estimated V_{cmax} and J_{max} was compared against a set of measurements of P_{sat} not used in the parameter estimation. The input environmental variables were PPFD (1,500 μmol m^{-2} s^{-1}) and leaf temperature (5–30°C) for each climatic treatment and water regime during GP-I and GP-II. As shown in Fig. 5, the modeled P_{sat} generally coincided well with the measured P_{sat}. Nevertheless, some discrepancies between the modeled and measured photosynthesis were still found, especially in ET.

Discussion and conclusions

Effects of climatic treatments: The phenological phase and developmental stage of RCG plants are triggered by thermal time (Sahramaa and Jauhiainen 2003). In the study site of boreal zone, the atmospheric temperature was still comparatively cool during earlier summer. Elevated growth temperature could create a moderate environment for early development and growth of plants (Ge *et al*. 2012). During the early growing period, temperature-induced acceleration in plant development resulted in a higher photosynthetic rate under warmer temperature. However, the continuous warming induced earlier plant senescence, leading to decreases in chlorophyll content and photosynthetic capacity during the late growing stages (Ge *et al*. 2011, Zhou *et al*. 2011).

In this study, we found a similar variation of the photosynthetic parameters (V_{cmax} and J_{max}) for two growing periods. During the early growing period, warmer growth temperature increased V_{cmax} and J_{max} when measured at higher measurement temperatures. This reflected that the activation state of Rubisco in response to higher measurement temperature under warmer environment might be better than that under ambient growth temperature. This also resulted in a higher optimum temperature for photosynthesis under elevated growth temperature. At lower measurement temperatures, P_{sat} and V_{cmax} were slightly lower under elevated growth temperature compared to ambient growth temperature. It was because that the plants grown under warm environment tended to have less amounts of Rubisco and other enzymes for photosynthetic carbon metabolism than those grown under lower temperatures (Yamori *et al*. 2006, Urban *et al*. 2007). Thus, in such plants under high growth temperature, the photosynthesis performance at lower measurement temperatures was usually reduced (von Caemmerer and Quick 2000).

Later in the growing season, a continuous high temperature decreased the activation state (enthalpy of activation, ΔH_a) of Rubisco in plants (Table 3), resulting in a lower V_{cmax} with less sensitivity to the measurement conditions compared to ambient growth temperature, also due to earlier plant senescence. This was in agreement with the reports by Crafts-Brandner and Salvucci (2000) and Salvucci and Crafts-Brandner (2004). The response of J_{max} to elevated growth temperature was, in this work, similar to that for V_{cmax}. Both the photosynthetically active radiation absorbed by the leaves and the activity of the RuBP regeneration system may largely limit the rate of RuBP regeneration and determine the temperature dependence of J_{max} (Hikosaka 2005, Hikosaka *et al*. 2006). However, it is still unclear which components determine the temperature dependence of J_{max} by gas-exchange measurements alone.

Under a long-term elevation of CO_2, downward acclimation is usually observed in photosynthetic parameters, with several hypotheses being proposed to explain this phenomenon (Long *et al*. 2004, Ainsworth and Rogers 2007). On average, a 10% reduction of V_{cmax} and J_{max} in grasses and crops (Ainsworth and Rogers 2007, Zhang *et al*. 2009) has been reported along with a decrease in leaf nitrogen and Rubisco concentration (Nowak *et al*. 2004, Rogers *et al*. 2006, Pérez *et al*. 2007). One of the explanations is based on the re-allocation of nitrogen in the leaves (Wullschleger *et al*. 2002a,b). The shift of nitrogen from Rubisco towards RuBP regeneration would enable plants to reduce Rubisco content at high CO_2 level and to optimize their investment in photosynthetic machinery (Drake *et al*. 1997). Our results on the degree of decreases in V_{cmax} and J_{max} inferred that Rubisco activity

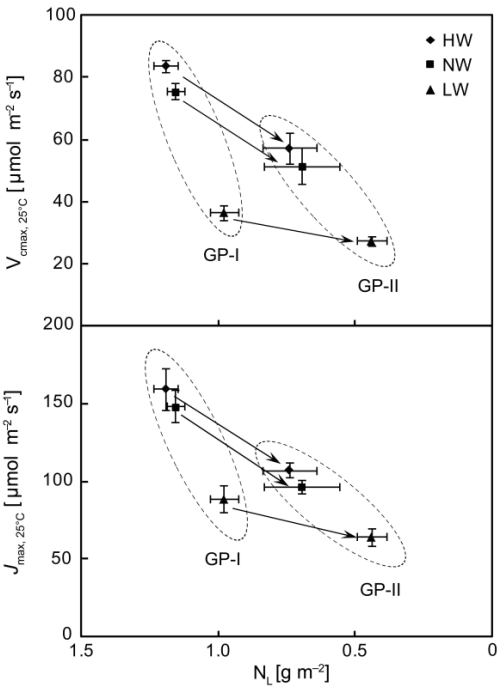

Fig. 4. Changes of the mean (± SE, *n*=4) leaf nitrogen concentration (N_L, reversed coordinate), and the mean (± SE, *n*=4) maximum rate of ribulose-1,5-bisphosphate carboxylase/oxygenase activity (V_{cmax}) and the mean (± SE, *n*=4) potential rate of electron transport (J_{max}) at 25°C from GP-I to GP-II, under different water regimes averaged by the climate treatments.

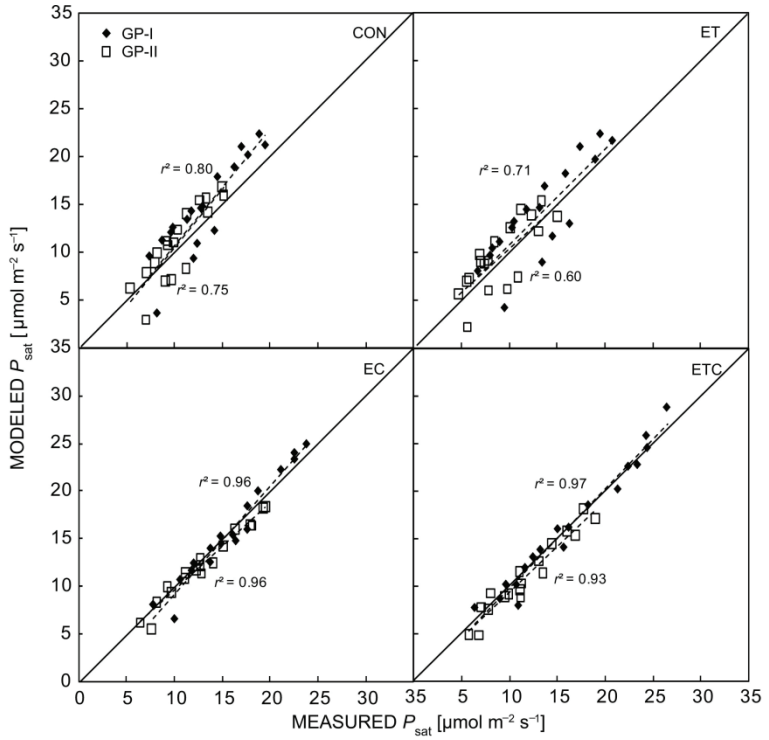

Fig. 5. Comparison of the predicted light-saturated net photosynthetic rates (P_{sat}) with the measurements by the fully parameterized model (Eqs. 1–6) in the CON, ET, EC and ETC chambers at different measurement temperatures (5–30°C) during GP-I and GP-II (dashed line), over the water regimes. Curve was fitted with linear function with coefficient of determination (r^2). The measured P_{sat} was not used for the estimation of the model parameters.

was reduced under elevated CO_2 more than the capacity for RuBP regeneration.

During the early growing period, it was found that elevated growth temperature increased the photosynthesis in ETC compared to EC. In spring time, a warmer growth temperature may accelerate the carboxylation of Rubisco due to earlier development (Alonso *et al*. 2008, 2009). However, a continuous high temperature will inhibit the activity of Rubisco (Schrader *et al*. 2006). As our previous study, the temperature-induced earlier senescence offset the effect of "CO_2 fertilization" during the late stage of growing season (Ge *et al*. 2012).

Effects of water regimes: As measured in this work, low soil water availability reduced the stomatal conductance, thus limiting the CO_2 diffusion to intercellular space with the reduction in carbon uptake and biomass growth, as presented by Zhou *et al*. (2011). In this work, water stress shifted the optimum temperature for photosynthesis to lower temperatures, probably as a result of biochemical impairments such as decreasing photosynthetic enzyme activity and regeneration (Flexas *et al*. 2004a,b; 2006a,b). Moreover, the optimum temperature for photosynthesis and activity of biochemical enzyme is dependent on yield of photosystem center. As reported in our previous study (Ge *et al*. 2011), the effective photochemical efficiency and electron transport rate in photosystem center exhibited negative responses to water shortage, indicating a reduced efficiency of excitation energy or a damage in the center.

For two growing periods, soil water availability affected the variation in photosynthesis and biochemical parameters much more than climatic treatment did. Compared to well-watered conditions, LW significantly decreased V_{cmax} and J_{max} across measurement temperatures and growing periods, providing further evidence that not only diffusive conductance but also intrinsic photosynthetic capacity was limited, which had been frequently found in other studies (Flexas *et al*. 2004a, 2006a,b; Hu *et al*. 2010). The limitation of the photosynthetic response to water stress could be attributed to a decrease in Rubisco activity (Flexas *et al*. 2004a, 2006a,b; Zhou *et al*. 2007, Hu *et al*. 2010). As estimated in this work, ΔH_a was significantly reduced in LW compared to HW and NW (Table 3). Also, the nonactivation of other enzymes in the Calvin cycle or a decrease in ATP and RuBP synthesis could be behind this result (Lawlor 2002, Parry *et al*. 2002). The limitation of J_{max}, indicating a down-regulation of electron transport and activity of soluble enzymes of the stroma, is among the earliest responses of plants to water stress (Flexas *et al*. 2004b, Zhou *et al*. 2007, Hu *et al*. 2010). Nevertheless, it is uncertain which process is the most sensitive to drought.

Our results indicated that the photosynthetic parameters acclimated to the seasonal degradation of leaf nitrogen content, representing a descent trajectory, regardless of climatic treatment and water regime. This is because the photosynthetic capacity is closely linked to nitrogen through the nitrogen-rich enzyme of Rubisco. The leaf nitrogen content of RCG plants in LW was much lower than that in HW and NW during both growing stages, leading to a "flat" decline trend of photosynthetic parameters through the growing season. However, this

combined reduction in the biochemical parameters and leaf nitrogen content might reflect a cooperated adjusting mechanism regarding the self-protection of enzyme and nitrogen allocation under drought conditions (Hu *et al*. 2010).

Interactive effects of water availability and climatic treatment: Our results showed a further adverse effect of soil drought on photosynthesis with lower V_{cmax} and J_{max}, especially under high temperature, suggesting that water stress aggravated the effects of high temperature, and their combination had a more detrimental effect than either drought or high temperature alone. This was in agreement with the results of Aranjuelo *et al*. (2005) and Xu and Zhou (2006), who demonstrated that a continuous high temperature can affect more drastically the activity of biochemical enzyme and integrity of photosystem center because cumulative effects can intensify the negative response to drought. Our previous results also reflected that water stress exacerbated the adverse effects of high temperature on photosystem function (Ge *et al*. 2011).

The mitigation effect of elevated CO_2 on photosynthesis of RCG plants under low soil water availability due to decreased stomatal conductance, and the consequent reduced water loss, can be detected (Zhou *et al*. 2011). However, our results implied that the magnitude of photosynthetic acclimation in elevated CO_2 is not altered by water availability, which was in agreement with the measurements by Aranjuelo *et al*. (2005). Nevertheless, the modification of V_{cmax} and J_{max}, representing Rubisco carboxylation efficiency and RuBP regeneration, under interaction of water stress and CO_2 enrichment is not well understood, and more investigations are still required.

Performance of photosynthesis model: Over two growing stages, the linear regression for the relationship between observed and predicted photosynthesis was not significantly different from the 1:1 line. However, there were still some discrepancies. One of the reasons was the usage of the same C_c in the calculations, potentially leading to an overestimation of photosynthesis at lower measurement temperatures and underestimation at higher ones. Furthermore, the stomatal conductance was not constrained depending on the environmental factors such as vapor pressure deficit and soil moisture, for the photosynthesis calculations. Nevertheless, the photosynthesis model with the biochemical parameters estimated from two growing periods was able to fairly describe the temperature response of photosynthesis under climatic treatments and water regimes.

References

Ainsworth, E.A., Rogers, A.: The response of photosynthesis and stomatal conductance to rising (CO_2): mechanisms and environmental interactions. – Plant Cell Environ. **30**: 258-270, 2007.

Alonso, A., Pérez, P., Morcuende, R., Martínez-Carrasco, R.: Future CO_2 concentrations, though not warmer temperatures, enhance wheat photosynthesis temperature responses. – Physiol. Plant. **132**: 102-112, 2008.

Alonso, A., Pérez, P., Martínez-Carrasco, R.: Growth in elevated CO_2 enhances temperature response of photosynthesis in wheat. – Physiol. Plant. **135**: 109-120, 2009.

Aranjuelo, I., Pérez, P., Hernández, L., Irigoyen, J.J., Zita, G., Martínez-Carrasco, R., Sánchez-Díaz, M.: The response of nodulated alfalfa to water supply, temperature and elevated CO_2: photosynthetic down-regulation. – Physiol. Plant. **123**: 348-358, 2005.

Bernacchi, C.J., Singsaas, E.L., Pimentel, C., Portis, A.R., Long, S.P.: Improved temperature response functions for models of Rubisco-limited photosynthesis. – Plant Cell Environ. **24**: 253-259, 2001.

Bernacchi, C.J., Portis, A.R., Nakano, H., von Caemmerer, S., Long, S.P.: Temperature response of mesophyll conductance. Implications for the determination of Rubisco enzyme kinetics and for limitations to photosynthesis *in vivo*. – Plant Physiol. **130**: 1992-1998, 2002.

Crafts-Brandner, S.J., Salvucci, M.E.: Rubisco activase constrains the photosynthetic potential of leaves at high temperature and CO_2. – Proc. Natl. Acad. Sci. USA **97**: 13430-13435, 2000.

Drake, B.G., González-Meler, M.A., Long, S.P.: More efficient plants: a consequence of rising atmospheric CO_2? – Annu. Rev. Plant Physiol. Mol. Biol. **48**: 609-639, 1997.

Farquhar, G.D., von Caemmerer, S., Berry, J.A.: A biochemical model of photosynthetic CO_2 assimilation in leaves of C_3 species. – Planta **149**: 78-90, 1980.

Farquhar, G.D., von Caemmerer, S.: Modelling of photosynthetic responses to environmental conditions. – In: Lange, O.L., Nobel, P.S., Osmond, C.B., Ziegler, H. (ed.): Physiological Plant Ecology. II. Encyclopedia of Plant Physiology. Vol. 12B. Pp. 548-577. Springer-Verlag, Berlin 1982.

Flexas, J., Bota, J., Loreto, F., Cornic, G., Sharkey, T.D.: Diffusive and metabolic limitations to photosynthesis under drought and salinity in C_3 plants. – Plant Biol. **6**: 269-279, 2004a.

Flexas, J., Bota, J., Cifre, J., Escalona, J.M., Galmes, J., Gulias, J., Lefi, E.K., Martinez-Canellas, S.F., Moreno, M.T., Ribas-Carbo, M., Riera, D., Sampol, B., Medrano, H.: Understanding down-regulation of photosynthesis under water stress: future prospects and searching for physiological tools for irrigation management. – Ann. Appl. Biol. **144**: 273-283, 2004b.

Flexas, J., Bota, J., Galmés, J., Medrano, H., Ribas-Carbo, M.: Keeping a positive carbon balance under adverse conditions: responses of photosynthesis and respiration to water stress. – Physiol. Plant. **127**: 343-352, 2006a.

Flexas, J., Ribas-Carbo, M., Bota, J., Galmés, J., Henkle, M., Martinez-Canellas, S., Medrano, H.: Decreased Rubisco activity during water stress is not induced by decreased relative water content but related to condition of low stomatal conductance and chloroplast CO_2 concentration. – New Phytol. **172**: 73-82, 2006b.

Ge, Z.M., Zhou, X., Kellomäki, S., Wang, K.Y., Peltola, H., Martikainen, P.J.: Responses of leaf photosynthesis, pigments and chlorophyll fluorescence within canopy position in

a boreal grass (*Phalaris arundinacea* L.) to elevated temperature and CO_2 under varying water regimes. – Photosynthetica **49**: 172-184, 2011.

Ge, Z.M., Zhou, X., Biasi, C., Kellomäki, S., Wang, K.Y., Peltola, H., Martikainen, P.J.: Carbon assimilation and allocation (^{13}C labeling) in a boreal perennial grass (*Phalaris arundinacea*) subjected to elevated temperature and CO_2 through a growing season. – Environ. Exp. Bot. **75**: 150-158, 2012.

Gouasmi, M., Mordelet, P., Demarez, V., Gastellu-Etchegorry, J.P., Le Dantec, V., Dedieu, G., Menaut, J.C., Calvet, J.C., Lamaze, T.: Photosynthesis of a temperate fallow C3 herbaceous ecosystem: measurements and model simulations at the leaf and canopy levels. – Photosynthetica **47**: 331-339, 2009.

Hikosaka, K.: Nitrogen partitioning in the photosynthetic apparatus of Plantago asiatica leaves grown under different temperature and light conditions: similarities and differences between temperature and light acclimation. – Plant Cell Physiol. **46**: 1283-1290, 2005.

Hikosaka, K., Ishikawa, K., Borjigidai, K., Muller, O., Onoda, Y.: Temperature acclimation of photosynthesis: mechanisms involved in the changes in temperature dependence of photosynthetic rate. – J. Exp. Bot. **57**: 291-302, 2006.

Hu, L.X., Wang, Z.L., Huang, B.R.: Diffusion limitations and metabolic factors associated with inhibition and recovery of photosynthesis from drought stress in a C_3 perennial grass species. – Physiol. Plant. **139**: 93-106, 2010.

Lawlor, D.W.: Limitation to photosynthesis in water-stressed leaves: stomata vs. metabolism and the role of ATP. – Ann. Bot. **89**: 1-15, 2002.

Long, S.P., Bernacchi, C.J.: Gas exchange measurements, what can they tell us about the underlying limitations to photosynthesis? Procedures and sources of error. – J. Exp. Bot. **54**: 2393-2401, 2003.

Long, S.P., Ainsworth, E.H., Rogers, A., Ort, D.R.: Rising atmospheric carbon dioxide: plants FACE the future. – Annu. Rev. Plant. Biol. **55**: 591-628, 2004.

Medlyn, B.E., Loustau, D., Delzon, S.: Temperature response of parameters of a biochemically based model of photosynthesis. I. Seasonal changes in mature maritime pine (*Pinus pinaster* Ait.). – Plant Cell Environ. **25**: 1155-1165, 2002a.

Medlyn, B.E., Dreyer, E., Ellsworth, D., Forstreuter, M., Harley, P.C., Kirschbaum, M.U.F., Le Roux, X., Montpied, P., Stassenmeyer, J., Walcroft, A., Wang, K., Loustau, D.: Temperature response of parameters of a biochemically based model of photosynthesis. II. A review of experimental data. – Plant Cell Environ. **25**: 1167-1179, 2002b.

Nowak, R.S., Ellsworth, D.S., Smith, S.D.: Functional responses of plants to elevated atmospheric CO_2 – do photosynthetic and productivity data from FACE experiments support early predictions? – New Phytol. **162**: 253-280, 2004.

Parry, M.A., Andraloj, P.J., Khan, S., Lea, P.J., Keys, A.J.: Rubisco activity: effects of drought stress. – Ann. Bot. **89**: 833-839, 2002.

Pérez, P., Zita, G., Morcuende, R., Martínez-Carrasco, R.: Elevated CO_2 and temperature differentially affect photosynthesis and resource allocation in flag and penultimate leaves of wheat. – Photosynthetica **45**: 9-17, 2007.

Rogers, A., Gibon, Y., Stitt, M., Morgan, P.B., Bernacchi, C.J., Ort, D.R., Long, S.P.: Increased C availability at elevated carbon dioxide concentration improves N assimilation in a legume. – Plant Cell Environ. **29**: 1651-1658, 2006.

Salvucci, M.E., Crafts-Brandner, S.J.: Inhibition of photosynthesis by heat stress: the activation state of Rubisco as a limiting factor in photosynthesis. – Physiol. Plant. **120**: 179-186, 2004.

Sahramaa, M., Jauhiainen, L.: Characterization of development and stem elongation of reed canary grass under northern conditions. – Ind. Crop Prod. **18**: 155-169, 2003.

Schrader, S.M., Kane, H.J., Sharkey, T.D., von Caemmerer, S.: High temperature enhances inhibitor production but reduces fallover in tobacco Rubisco. Funct. Plant Biol. **33**: 921-929, 2006.

Sharkey, T.D., Bernacchi, C.J., Farquhar, G.D., Singsaas, E.L.: Fitting photosynthetic carbon dioxide response curves for C_3 leaves. – Plant Cell Environ. **30**: 1035-1040, 2007.

Urban, O., Ač, A., Kalina, J., Priwitzer, T., Šprtová, M., Špunda, V., Marek, M.V. Temperature dependences of carbon assimilation processes in four dominant species from mountain grassland ecosystem. – Photosynthetica **45**: 392-399, 2007.

von Caemmerer, S., Quick, P.W.: Rubisco, physiology *in vivo*. – In: Leegood, R.C., Sharkey, T.D., von Caemmerer, S. (ed.): Photosynthesis: Physiology and Metabolism. Pp. 85-113. Kluwer Academic Publ., Dordrecht 2000.

Wullschleger, S.D., Gunderson, C.A., Hanson, P.J., Wilson, K.B., Norby, R.J.: Sensitivity of stomatal and canopy conductance to elevated CO_2 concentration – interacting variables and perspectives of scale. – New Phytol. **153**: 485-496, 2002a.

Wullschleger, S.D., Tschaplinski, T.J., Norby, R.J.: Plant water relations at elevated CO_2 – implications for water-limited environments. – Plant Cell Environ. **25**: 319-331, 2002b.

Yamori, W., Suzuki, K., Noguchi, K., Nakai, M., Terashima, I.: Effects of Rubisco kinetics and Rubisco activation state on the temperature dependence of the photosynthetic rate in spinach leaves from contrasting growth temperatures. – Plant Cell Environ. **29**: 1659-1670, 2006.

Zhang, D.Y., Chen, G.Y., Chen, J., Yong, Z.H., Zhu, J.G., Xu, D.Q.: Photosynthetic acclimation to CO_2 enrichment related to ribulose-1,5-bisphosphate carboxylation limitation in wheat. – Photosynthetica **47**: 152-154, 2009.

Zhou, Y., Lam, H.M., Zhang, J.: Inhibition of photosynthesis and energy dissipation induced by water and high light stresses in rice. – J. Exp. Bot. **58**: 1207-1217, 2007.

Zhou, X., Ge, Z.M., Kellomäki, S., Wang, K.Y., Peltola, H., Martikainen, P.: Effects of elevated CO_2 and temperature on leaf characteristics, photosynthesis and carbon storage in aboveground biomass of a boreal bioenergy crop (*Phalaris arundinacea* L.) under varying water regimes. – Global Change Biol. Bioenerg. **3**: 223-234, 2011.

Zhou, X., Ge, Z.M., Kellomäki, S., Wang, K.Y., Peltola, H., Martikainen, P., Lemettinen, M., Hassinen, A., Ikonen, R.: Multi-objective environment chamber system for studying plant responses to climate change. – Photosynthetica DOI: 10.1007/s11099-011-0063-6, 2012.

Xu, Z.Z, Zhou, G.S.: Combined effects of water stress and high temperature on photosynthesis, nitrogen metabolism and lipid peroxidation of a perennial grass *Leymus chinensis*. – Planta **224**: 1080-1090, 2006.

Appendix

In the photosynthesis model, the rate of net photosynthesis is limited by the slowest of the two following processes: the Rubisco-limited rate of photosynthesis (P_c) and the RuBP-regeneration-limited rate of photosynthesis (P_j), considering the regulation by g_m and C_c (CO_2 concentration in the chloroplast) as follows:

$$P_N = \min\left(P_c, P_j\right) \tag{1}$$

$$C_c = C_i - P_N/g_m \tag{2}$$

With the P_N-C_i curves, the C_c can be estimated using the g_m (Bernacchi *et al*. 2002).

The Rubisco-limited photosynthesis is given by:

$$P_c = V_{cmax}\left[\frac{C_c - \Gamma^*}{C_c + K_c(1 + O/K_o)}\right] - R_d \tag{3}$$

where V_{cmax} is the maximum rate of carboxylation, Γ^* is the CO_2 compensation point in the absence of dark respiration, K_c and K_o are the Michaelis constants for CO_2 and O_2, respectively, and O is the oxygen concentration. Γ^* is a function of the CO_2/O_2 specificity (K_oV_c/K_cV_o) and O, and V_o taken as $0.21V_c$ (Farquhar *et al*. 1980). The temperature dependencies of K_c and K_o used in this study were the same as those used by Bernacchi *et al*. (2001, 2002).

Similar to Eq. 3, the RuBP-limited photosynthesis rate is:

$$P_j = J\left[\frac{C_c - \Gamma^*}{4\,C_c + 8\,\Gamma^*}\right] - R_d \tag{4}$$

where J is the rate of electron transport. J is related to the irradiance, by:

$$J = \frac{\alpha\,\mathrm{PPFD} + J_{max} - \sqrt{\left(\alpha\,\mathrm{PPFD} + J_{max}\right)^2 - 4\,\theta\,\alpha\,\mathrm{PPFD}\,J_{max}}}{2\,\theta} \tag{5}$$

where θ (0.88) is the curvature of the PPFD response curve of J and α is the quantum efficiency.

The parameters of V_{cmax} and J_{max} estimated from the P_N-C_c and P_N-PPFD curves respond to measurement temperature gradient. The equations used here can be found in Sharkey *et al*. (2007):

$$V_{cmax}, J_{max} = \frac{\exp\left(c - \frac{\Delta H_a}{R\,T_l}\right)}{1 + \exp\left(\frac{\Delta S\,T_l - \Delta H_d}{R\,T_l}\right)} \tag{6}$$

where ΔH_a is the enthalpy of activation for CO_2 and PPFD-saturated assimilation, ΔH_d is the enthalpy of deactivation, ΔS is the entropy of the desaturation equilibrium of CO_2 and PPFD-saturated assimilation, R is the molar gas constant, T_l is leaf temperature, and c is a scaling constant.

The optimal temperature (T_{opt}) for photosynthesis was calculated as (Medlyn *et al*. 2002a):

$$T_{opt} = \frac{\Delta H_d}{\Delta S - R\ln[\Delta H_a/(\Delta H_d - \Delta H_a)]} \tag{7}$$